SSRG International Journal of Civil Engineering Volume 7 Issue 5, 10-20, May 2020
ISSN: 2348 – 8352 /doi:10.14445/23488352/IJCE-V7I5P102 ©2020 Seventh Sense Research Group®

Seismic Vibration Control of a Two-Way Asymmetric Tall Building Installed with Passive Viscous Dampers under Bi-Directional Excitations

Nisha J. Pandit [#1], Snehal V. Mevada [#2], Vishal B. Patel [#3]

[#1]*PG Research Scholar, Structural Engineering Department, Birla Vishvakarma Mahavidyalaya Engineering College, Vallabh Vidyanagar, Gujarat, India*

[#2,3]*Assistant Professor, Structural Engineering Department, Birla Vishvakarma Mahavidyalaya Engineering College, Vallabh Vidyanagar, Gujarat, India.*

Received Date: 08 April 2020
Revised Date: 22 May 2020
Accepted Date:28 May 2020

Abstract

The study focuses on the seismic vibration control of a two-way asymmetric, 20 storied building installed with various structural control systems such as passive linear viscous dampers (LVDs) and non-linear viscous dampers (NLVDs). The building is subjected to bi-directional seismic excitations of past earthquakes. The displacement, velocity and acceleration responses for the multi-storey asymmetric building are obtained by mathematically solving the governing equations of motion using the state space approach. Optimum parameters for the dampers are derived from the numerical study. To investigate the effectiveness of dampers in the asymmetric building, a comparative study between the controlled response and the corresponding uncontrolled response is carried out.

Moreover, the study is carried out to determine the optimum placement of dampers to be installed in the multi-storey building under consideration. Various response quantities such as top floor lateral-torsional displacement as well as acceleration at the centre of mass and storey displacement of the structure are obtained. For the present study, it is observed that lateral-torsional response quantities reduce significantly after the installation of LVDs and NLVDs.

Keywords —*Asymmetric Building, Seismic Response, Optimum, Viscous Dampers*

I. INTRODUCTION

Modern tall buildings use lightweight materials for construction. Hence, they are more flexible, which can lead to large earthquake-induced vibrations resulting in occupant discomfort and failures in the structure. Likewise, based on geometry, structures are classified into two categories, (i) Symmetric structures, (ii) Asymmetric structures. Asymmetric structures are further divided into one-way asymmetric structures and two-way asymmetric structures. Two-way asymmetric structures are extremely susceptible to severe damage during earthquakes. The uneven distribution of mass and stiffness leads to asymmetry in the structure which generates torsion. The major focus of the structural engineer is to decrease the torsional effects mainly by reducing the eccentricity. But in some cases, it is not feasible to reduce the asymmetry due to functional and architectural demands. Hence, in such cases, structural control devices play a key role in reducing the lateral-torsional response of structures. In the past, many researchers have investigated the performance of various structural control devices such as passive control, active control, semi-active control and hybrid control devices for reducing the lateral-torsional response of various structures.

Goel (1998) studied the effects of supplemental viscous damping on vibration control of the one-way asymmetric system and found that edge deformations in asymmetric systems can be reduced to a greater extent as compared to those in the corresponding symmetric systems [5]. Lin and Chopra (2002) studied the effectiveness of NLVDs for the elastic, single-storey symmetric system. It was shown that NLVDs are more effective in reducing response than LVDs with reduced damper force [10]. Rodrigo and Romero (2003) studied the seismic behaviour of a six-storey steel structure. They found that the maximum force experienced by the dampers in the non-linear case may be reduced more as compared to the linear retrofitting case with a similar structural seismic performance [13]. Lin and Chopra (2003) investigated the effects of the plan-wise distribution of fluid viscous dampers (FVDs) that determines the response of linear elastic, one-floor, asymmetric-plan systems [11]. Goel (2005) studied the seismic response of one-storey, one-way asymmetric linear and non-linear systems with non-linear fluid viscous dampers and proposed effects of non-linearity of dampers [6]. Mevada and Jangid (2012) investigated the effect of supplementary viscous damping on the response of the single-storey, one-way asymmetric system. They found that the response of building depends on the supplemental damping eccentricity ratio and eccentricity ratio [15]. Bahnasy and Lavan (2013) compared the seismic behaviour of structures optimally retrofitted with LVDs versus that of structures optimally retrofitted with NLVDs and proposed an optimal exponent value required for NLVDs installed in buildings of various heights [2]. Mehta and Mevada (2017) studied the seismic response of linearly elastic, single-storey, two-way asymmetric building installed with LVDs, NLVDs, semi-active friction dampers (SAFDs) and hybrid arrangement of dampers under bi-directional earthquake excitations [14]. Banazadeh et al. (2017) studied that using FVD improves the performance of the special moment-resisting frame (SMRF) and reduces its collapse probability in comparison with SMRF without dampers [3].

The above study highlights the effectiveness of passive and semi-active control systems for asymmetric buildings under earthquake excitation. However, less work has been done to investigate the effectiveness of viscous dampers in two-way asymmetric tall buildings subjected to bi-directional seismic excitations. In this paper, the seismic response of a 20 storied, two-way asymmetric building installed with LVDs and NLVDs subjected to bi-directional earthquakes is investigated. Further, the study is carried out to propose the optimum placement of dampers to be installed.

II. STRUCTURAL MODEL

The system considered is an idealised 20-storied building which consists of a rigid deck supported by structural elements. The following assumptions are made for the structural system under consideration:

- The floor of the superstructure is considered as rigid.
- Columns are axially rigid.
- The force-deformation relationship of the superstructure is considered as linear and within the elastic range.
- In stiffness matrix calculation, beam and slab stiffness are neglected.
- The mass of the slab is assumed to be consistently distributed, and thus the centre of mass (CM) coincides with the geometrical centre of the rigid floor slab.

Plan and elevation of the building are as shown in Fig. 1(a) and Fig. 1(b), respectively. Location and size of columns are considered in such a way that it produces the stiffness asymmetry concerning CM in x-direction and y-direction. Thus, the centre of rigidity (CR) is located at an eccentric distance e_x from the CM in the x-direction and an eccentric distance e_y from CM in the y-direction. The building considered consists of three degrees of freedom at each storey, namely the lateral displacement in the x-direction (u_x), lateral displacement in the y-direction (u_y), and rotational displacement (u_θ). Edge of building nearer to CR and the edge farther to CR is referred to the as stiff edge and flexible edge, respectively.

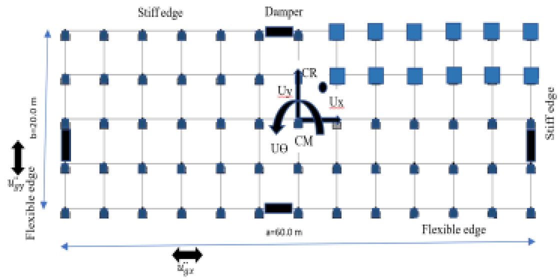

Fig. 1(a)

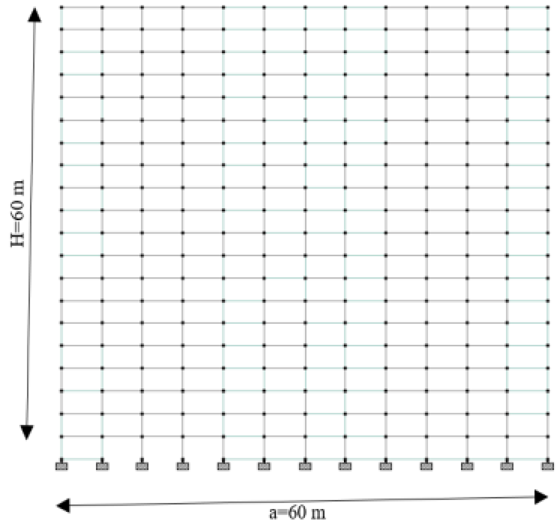

Fig. 1(b)

Fig. 1 (a) Plan of two-way asymmetric 20 storied building (b) Elevation of two-way asymmetric 20 storied building

III. SOLUTION OF EQUATIONS OF MOTION

The governing equation of motion of the building is mentioned in matrix form in equation (1), where M, C and K are the mass matrix, damping matrix and stiffness matrix of the building, respectively; $u = \{u_x\, u_y\, u_\theta\}^T$ is the displacement vector; $\dot{u} = \{\dot{u}_x\, \dot{u}_y\, \dot{u}_\theta\}^{\mathrm{T}}$ is the velocity vector; $\ddot{u} = \{\ddot{u}_x\, \ddot{u}_Y\, \ddot{u}_\theta\}^{\mathrm{T}}$ is the acceleration vector; Γ is the influence coefficient vector; $\ddot{u}_g = \{\ddot{u}_{gx}\, \ddot{u}_{gy}\, \ddot{u}_{g\theta}\}^{\mathrm{T}}$ ground acceleration vector, where $\ddot{u}_{g\theta}$ is considered zero for the present study; Λ is the damper location matrix which depends on the location of dampers; $F = \{F_{dx}F_{dy}F_{d\theta}\}^{\mathrm{T}}$ is the vector of control forces;

F_{dx}, F_{dy} and $F_{d\theta}$ are resultant control forces of damper along two lateral and rotational direction, respectively.

$$\mathrm{M\ddot{u} + C\dot{u} + Ku = -M\Gamma \ddot{u}_g + \wedge F} \tag{1}$$

The mass matrix M can be expressed as shown in equation (2), where m represents lumped mass of the deck; and r is the mass-radius of gyration about the vertical axis through CM and is given by, $r = \sqrt{\frac{a^2+b^2}{12}}$ where, a and b are plan dimension of the building.

$$M = \begin{pmatrix} M_1 & 0 & 0 & 0 & 0 \\ 0 & M_2 & 0 & 0 & 0 \\ 0 & 0 & M_3 & 0 & 0 \\ 0 & 0 & 0 & \ddots & 0 \\ 0 & 0 & 0 & 0 & M_{20} \end{pmatrix} \tag{2}$$

$$\text{where, } \mathrm{M_1, M_2, \ldots\ldots, M_{20}} = \begin{pmatrix} \mathrm{m} & 0 & 0 \\ 0 & \mathrm{m} & 0 \\ 0 & 0 & \mathrm{mr^2} \end{pmatrix}$$

The stiffness matrix K can be expressed, as shown in equation (3), where $k_{xx} = \sum_i k_{xi}$, $k_{yy} = \sum_i k_{yi}$ are the total lateral stiffness in x and y-direction, respectively [4].

$$K = \begin{pmatrix} K_1+K_2 & -K_2 & 0 & 0 & 0 \\ -K_2 & K_2+K_3 & -K_3 & 0 & 0 \\ 0 & -K_3 & \ddots & 0 & 0 \\ 0 & 0 & 0 & K_{19}+K_{20} & -K_{20} \\ 0 & 0 & 0 & -K_{20} & K_{20} \end{pmatrix} \tag{3}$$

$$\text{where, } \mathrm{K_1, K_2, \ldots\ldots K_{20}} = \begin{pmatrix} \mathrm{k_{xx}} & \mathrm{k_{yx}} & \mathrm{k_{\theta x}} \\ \mathrm{k_{xy}} & \mathrm{k_{yy}} & \mathrm{k_{\theta y}} \\ \mathrm{k_{x\theta}} & \mathrm{k_{y\theta}} & \mathrm{k_{\theta\theta}} \end{pmatrix}$$

$$k_{x\theta} = k_{\theta x} = \sum_i (y_i \times k_{xi}) \tag{4}$$

and

$$k_{y\theta} = k_{\theta y} = \sum_i (x_i \times k_{yi})$$

$$k_{yx} = k_{xy} = 0 \tag{5}$$

and

$$k_{\theta\theta} = \sum_i k_{xi} y_i^2 + k_{yi} x_i^2$$

In equation (4) and equation (5), $k_{\theta\theta}$ is torsional stiffness of building about a vertical axis at CM; k_{xi} and k_{yi} indicate the lateral stiffness of i^{th} column in x and y-direction, respectively; x_i and y_i are the x and y-coordinate distance of i^{th} column concerning CM respectively. The damping matrix of the building is not known explicitly, and it is constructed from the Rayleigh's damping considering mass and stiffness of the building considered. Damping matrix is given in equation (6), where α and β are coefficients that depend on the damping ratio of the first two vibration modes. For the present study, 5% damping is considered for both modes of vibration of the building.

$$\mathrm{C = \alpha M + \beta K} \tag{6}$$

The governing equations of motion are solved using the state space method, and it is written in equation (7), where $z = \{u\ \dot{u}\}^T$ is a state vector; A is the system matrix; B is distribution matrix of control force; E is the distribution matrix of excitation. These matrices are expressed as shown in equation (8), where, I *am* the identity matrix [7].

$$\mathrm{\dot{z} = Az + BF + E\ddot{u}_g} \tag{7}$$

$$A = \begin{bmatrix} 0 & I \\ -M^{-1}K & -M^{-1}C \end{bmatrix} \tag{8}$$

$$B = \begin{bmatrix} 0 \\ -M^{-1}\wedge \end{bmatrix} \text{and } E = \begin{bmatrix} 0 \\ \Gamma \end{bmatrix}$$

Equation (7) is discretised in the time domain, and the excitation and control forces are assumed to be constant within any time interval. The solution may be written in an incremental form as shown in equation (9), where, k denotes the time step; and $A_d = e^{A\Delta t}$ represent the discrete-time step system matrix with Δt as a time interval. The constant-coefficient matrices B_d and E_d are discrete-time counterparts of matrices B and E and can be written, as shown in equation (10) [12].

$$\mathrm{z_{k+1} = A_d z_k + B_d F_k + E_d \ddot{u}_{gk}} \tag{9}$$

$$\begin{aligned} B_d &= A^{-1}(A_d - I)\,B \\ E_d &= A^{-1}(A_d - I)\,E \end{aligned} \tag{10}$$

IV. MODELLING OF FLUID VISCOUS DAMPERS

Fluid viscous dampers operate on the principle of fluid flowing through an orifice which provides the force that resists the motion of the structure during a seismic event. Fig. 2(a) and Fig. 2(b) show the schematic diagram and mathematical model of a typical FVD, respectively.

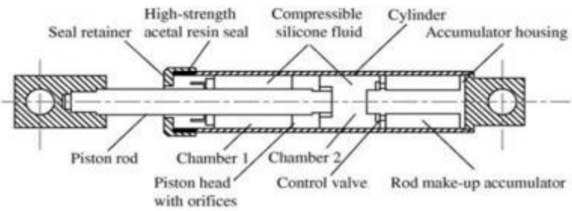

Fig. 2(a)

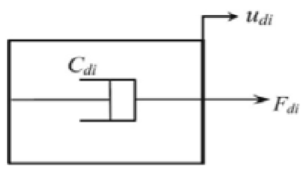

Fig. 2(b)

Fig. 2 (a) Schematic diagram of the FVD (b) Mathematical model of FVD

FVD consists of a cylindrical body and central piston which strokes through a fluid-filled chamber. The commonly used fluid is a silicone-based fluid which ensures proper performance and stability. Differential pressure generated across the piston head results in damper force.

$$F_i = C_{di}|\dot{u_{di}}|^{\alpha}\, sign(\dot{u_{di}}) \qquad (11)$$

The force in a viscous damper $F_i = (F_{af} or\ F_{ds})$ is proportional to the relative velocity between the ends of a damper and it is given by equation (11), where, C_{di} is damper coefficient of the i^{th} damper; $\dot{u_{di}}$ is the relative velocity between two ends of a damper which is to be considered; α is the power-law coefficient or damper exponent ranging from 0.1 to 1 for seismic applications and sign(·) is signum function. The design of piston head orifices primarily controls the value of the exponent. When α = 1, a damper is called as a linear viscous damper (LVD) and with the value of α smaller than unity, a damper will behave as a non-linear viscous damper (NLVD) [16].

V. NUMERICAL STUDY

Seismic response of a 20-storied, two-way asymmetric building installed with passive LVDs and NLVDs is investigated by numerical simulation using MATLAB. Parameters of the building are considered as per Table I.

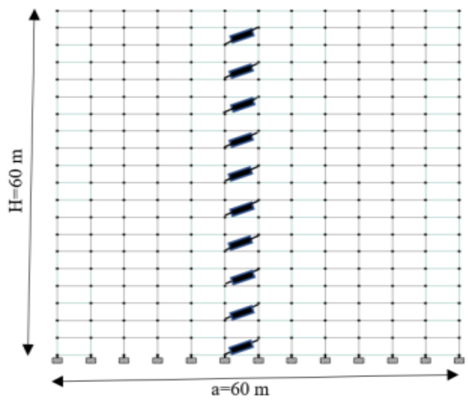

Fig. 3(a)

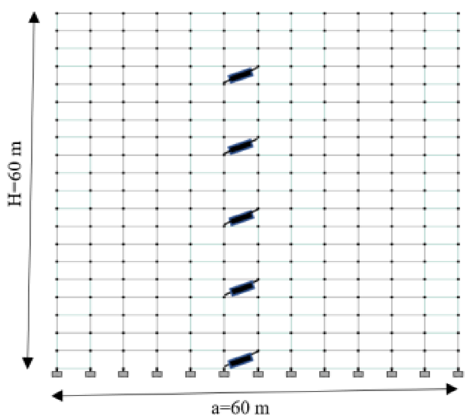

Fig. 3(b)

Fig. 3 (a) Configuration for 40 dampers (b) Configuration for 20 dampers

Total of four dampers is installed in one storey, as shown in Fig. 1(a). Further, to propose an optimum placement of dampers, a parametric study is carried out. Based on this study, the effectiveness of each model can be understood. As shown in Fig.3, two different configurations of damper location are studied namely,

- Four dampers arranged at each alternate odd storey and hence totalled 40 dampers are installed. Refer Fig. 3(a)
- Four dampers arranged at a three-storey interval and hence totaled 20 dampers are installed. Refer Fig. 3(b)

The response quantities of interest are; lateral-torsional displacements of floor mass obtained at the CM, lateral-torsional accelerations of floor mass obtained at the CM and storey displacements of the structure. Also, edge displacements; $u_{xf}, u_{xs}, u_{yf}, u_{ys}$ and edge velocities; $\dot{u_{xf}}, \dot{u_{xs}}, \dot{u_{yf}}, \dot{u_{ys}}$ are calculated to evaluate damper force. Based on the parametric study, optimum values C_d *and* α are calculated. Response quantities considered to evaluate the optimum value of C_d and α , are the maximum responses obtained at CM.

The responses are obtained by performing time history analysis under four different earthquake ground motions, namely, Imperial Valley (1940), Loma Prieta (1989), Northridge (1994) and Kobe (1995). The details of earthquakes such as peak ground acceleration (PGA), duration and recording station are summarised in Table II.

Table I

Building Parameters

Parameters	**Values**	**Units**
Plan dimension	60 x 20	m
Typical storey height	3	m
Columns on left side	650 x 650	mm
Columns at top right corner	850 x 850	mm
Beam	300 x 460	mm
Slab thickness	120	mm
Outer wall thickness	230	mm
Inner wall thickness	115	mm
Height of parapet wall	1	m
Total lumped mass	1.55×10^6	kg
e_x	4.59	m
e_y	1.97	m
Live load	2	kN/m^2
Grade of concrete	M 30	-
Grade of steel	Fe 500	-

To investigate the effectiveness of LVDs and NLVDs, the velocity exponent, α as expressed in equation (11). α is varied from 0.3 to 0.8 and damper coefficient, C_d is varied from $0\ to\ 50 \times 10^5$ N-sec/m for the case of 40 NLVDs and varied from $0\ to\ 90 \times 10^5$ N-sec/m for the case of 20 NLVDs.

Table II
Details of Earthquake Motions Considered for the Numerical Study

Earthquake	Recording station	Duration (sec)	PGA (g)	
			EQ_x	EQ_y
Imperial Valley, 1940	El Centro	40	0.31	0.21
Loma Prieta, 1989	Los Gatos Presentation Centre	25	0.96	0.59
Northridge, 1994	Sylmar Converter Station	40	0.89	0.61
Kobe, 1995	Japan Meteorological Agency	48	0.82	0.60

Fig. 4(a) to 4(f) and Fig. 5(a) to 5(f) show the effect of C_d and α on response parameters while using 40 NLVDs and 20 NLVDs respectively. These plots are derived for average values of response parameters generated from all the earthquakes considered. From Fig. 4, it is observed that, C_d increases and α decreases which leads to the reduction in all response quantities considered. No significant reduction is observed beyond the value of $C_d = 25 \times 10^5$ N-sec/m $and\ \alpha = 0.6$. Similarly, from Fig. 5 it is observed that optimum values of response quantities are obtained at $C_d = 50 \times 10^5$ N-sec/m and $\alpha = 0.6$.

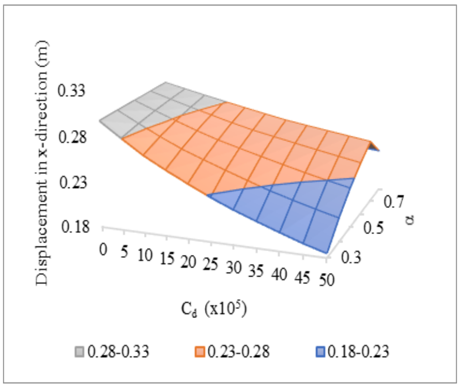

Fig. 4(a)

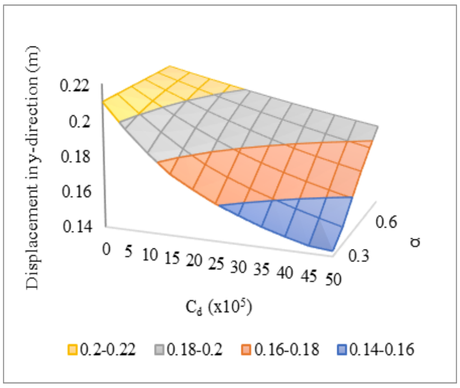

Fig. 4(b)

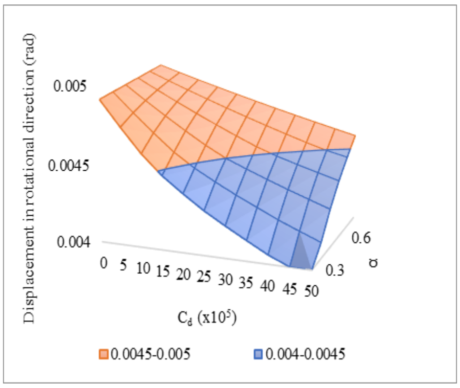

Fig. 4(c)

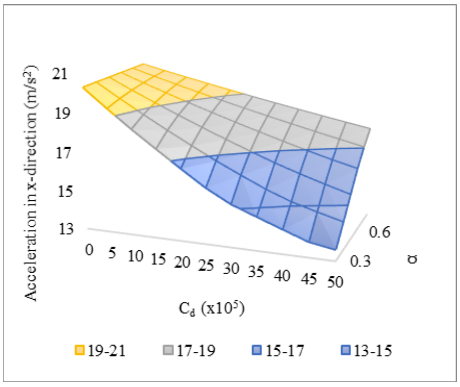

Fig. 4(d)

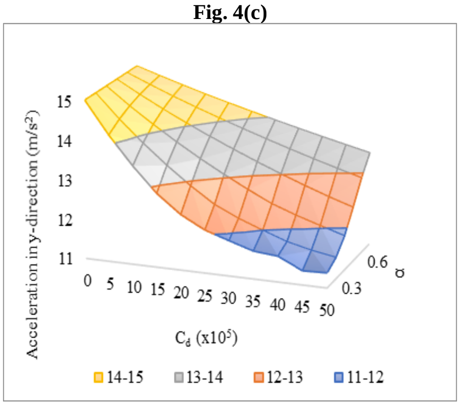

Fig. 4(e)

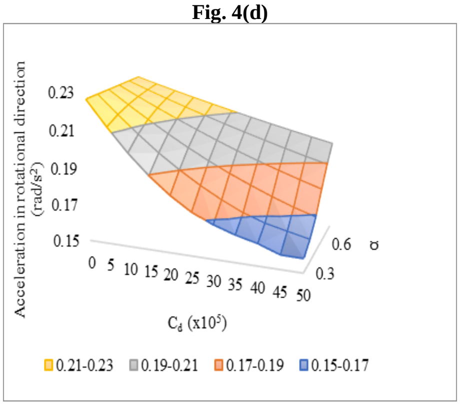

Fig. 4(f)

Fig. 4 Effect of α and C_d on response parameters for 40 NLVDs

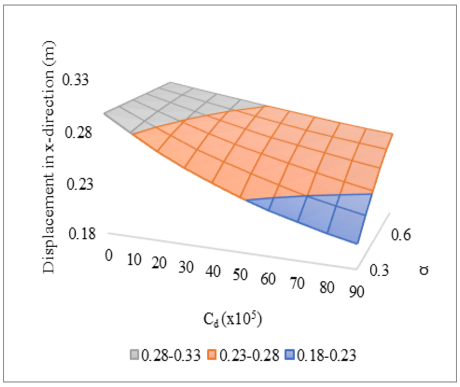

Fig. 5(a)

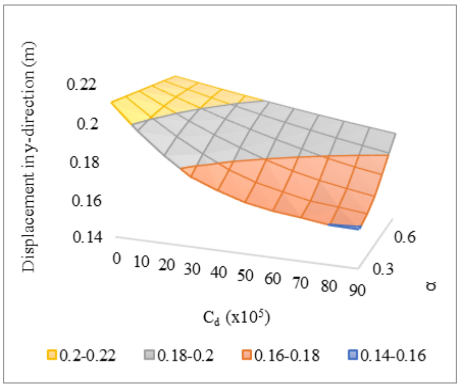

Fig. 5(b)

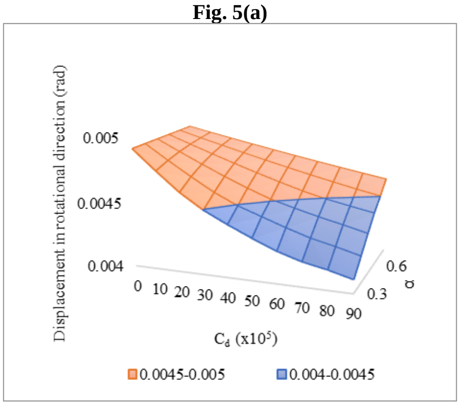

Fig. 5(c)

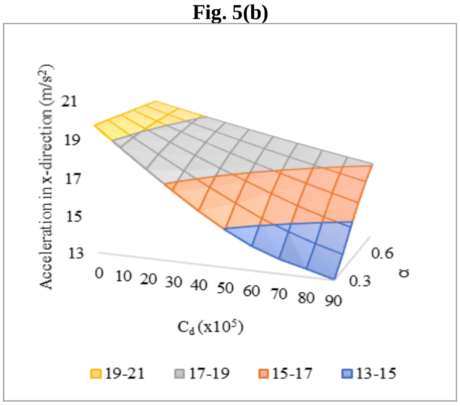

Fig. 5(d)

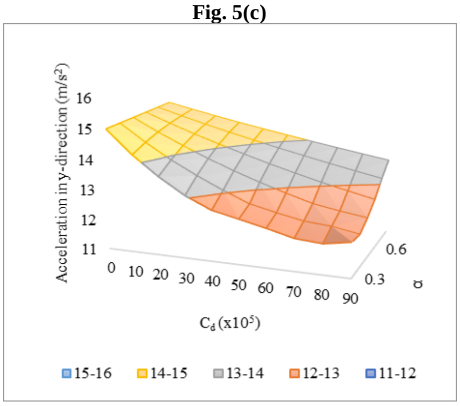

Fig. 5(e)

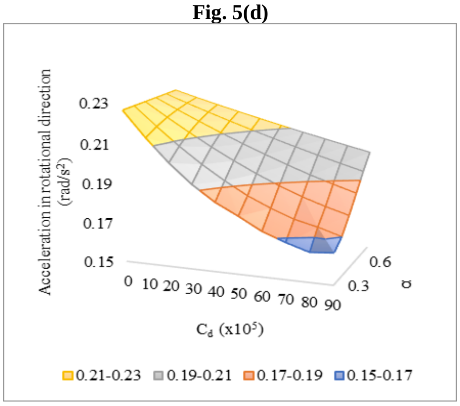

Fig. 5(f)

Fig. 5 Effect of α and C_d on response parameters for 20 NLVDs

Fig. 6(a) to 6(f) and Fig. 7(a) to 7(f) show the effect of C_d on response parameters while using 40 LVDs and 20 LVDs ($\alpha = 1.0$), respectively. For both the configuration of LVDs, C_d is varied from $0 \; to \; 30 \times 10^6$ N-sec/m, and it is observed that response parameters reduce as the value of C_d is increased. No significant reduction is observed beyond the value of $C_d = 20 \times 10^6$ N-sec/m.

Fig. 8 shows the damper force-displacement and damper force-velocity relationship for NLVDs. In contrast, Fig. 9 shows the damper force-displacement and damper force-velocity relationship for LVDs installed at the flexible edge for both the configurations (i.e. 40 dampers and 20 dampers) under Loma Prieta, 1989 earthquake. It shows the hysteresis loop, which indicates the dissipation of energy and reflects the behaviour of damper.

Fig. 8(a) shows that for the case of 40 NLVDs, energy dissipated at the flexible edge in the x-direction is 3.66×10^3 J. Similarly, Fig. 8(b) shows that for the case of 20 NLVDs, energy dissipated at the flexible edge in the x-direction is 1.35×10^3J. Fig. 9(a) shows that for the case of 40 LVDs, energy dissipated at the flexible edge in the x-direction is 8.25×10^2 J. Similarly, Fig. 9(b) shows that for the case of 20 LVDs, energy dissipated at the flexible edge in the x-direction is 1.53×10^3J.

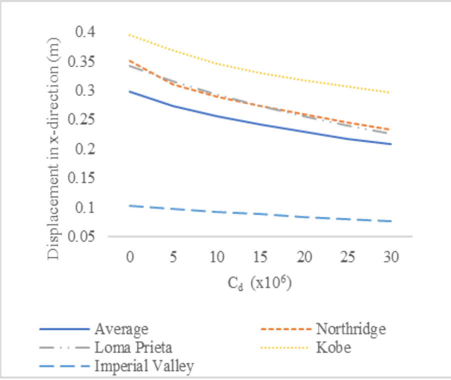

Fig. 6(a)

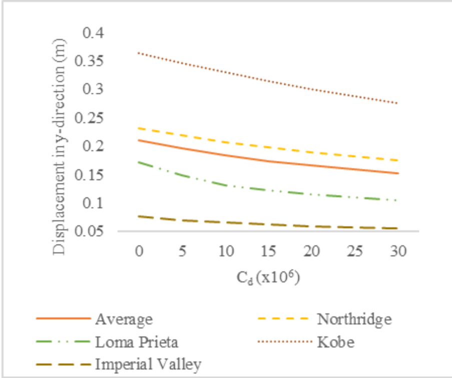

Fig. 6(b)

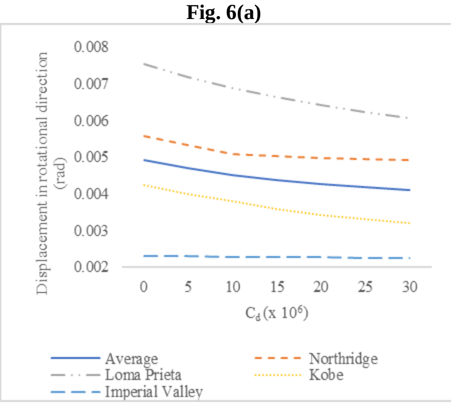

Fig. 6(c)

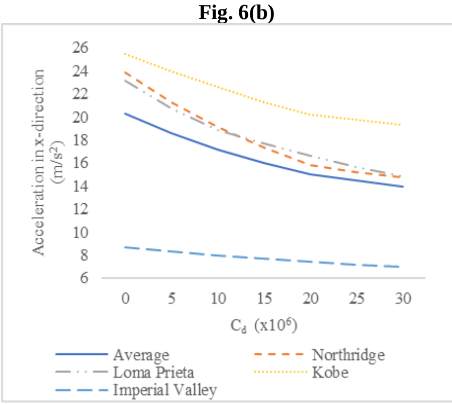

Fig. 6(d)

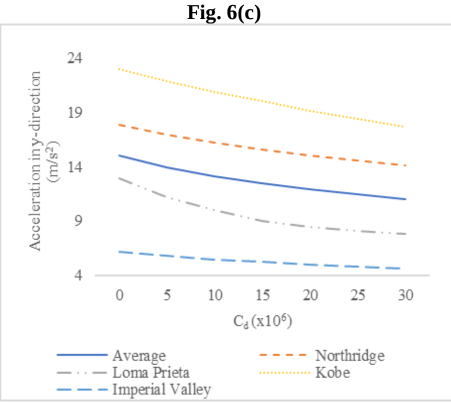

Fig. 6(e)

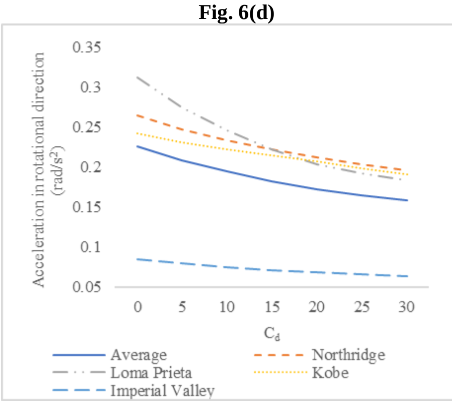

Fig. 6(f)

Fig. 6 Effect of C_d on response parameters for 40 LVDs

Table III

Response Quantities for Various Control Systems under Four Earthquakes

Response	**Control System**	**Imperial Valley, 1940**	**Loma Prieta, 1989**	**Northridge, 1994**	**Kobe, 1995**	**Average per cent reduction**
$\mathbf{u_x}$ (m)	Uncontrolled	0.1017	0.3411	0.3512	0.3941	-
	40 LVDs	0.0832 (18.3)	0.2548 (25.3)	0.2588 (26.3)	0.3177 (19.4)	22.3
	40 NLVDs	0.0918 (9.8)	0.3038 (10.9)	0.2977 (15.3)	0.3599 (8.7)	11.2
	20 LVDs	0.0919 (9.7)	0.2927 (14.2)	0.2889 (17.3)	0.3456 (12.3)	13.4
	20 NLVDs	0.0920 (9.6)	0.3045 (10.7)	0.2982 (15.1)	0.3606 (8.5)	11.0
$\mathbf{u_y}$ (m)	Uncontrolled	0.0763	0.1711	0.2318	0.3627	-
	40 LVDs	0.0595 (22.0)	0.1153 (32.6)	0.1894 (18.3)	0.3005 (17.2)	22.5
	40 NLVDs	0.0641 (15.9)	0.1357 (20.7)	0.2083 (10.1)	0.3376 (6.9)	13.4
	20 LVDs	0.0660 (13.5)	0.1315 (23.2)	0.2072 (10.6)	0.3295 (9.2)	14.1
	20 NLVDs	0.0643 (15.7)	0.1363 (20.4)	0.2085 (10.0)	0.3382 (6.8)	13.2
$\mathbf{u_\theta}$ (rad)	Uncontrolled	0.0023	0.0075	0.0056	0.0042	-
	40 LVDs	0.0023 (0.0)	0.0064 (14.8)	0.0050 (10.8)	0.0034 (19.6)	11.8
	40 NLVDs	0.0023 (0.0)	0.0070 (7.4)	0.0052 (7.4)	0.0039 (7.3)	5.7
	20 LVDs	0.0023 (0.0)	0.0069 (8.6)	0.0051 (8.7)	0.0038 (10.6)	7.3
	20 NLVDs	0.0023 (0.0)	0.0070 (7.3)	0.0052 (7.4)	0.0040 (7.1)	5.5

Response	Control System	Imperial Valley, 1940	Loma Prieta, 1989	Northridge, 1994	Kobe, 1995	Average per cent reduction
$\ddot{u}_x$ (m/s^2)	Uncontrolled	8.6507	23.161	23.883	25.434	-
	40 LVDs	7.4381 (14.0)	16.607 (28.3)	15.839 (33.7)	20.224 (20.5)	24.1
	40 NLVDs	8.1135 (6.2)	20.187 (12.8)	20.497 (14.2)	23.667 (7.0)	10.1
	20 LVDs	8.0508 (6.9)	18.900 (18.4)	19.120 (19.9)	22.560 (11.3)	14.1
	20 NLVDs	8.1637 (5.6)	20.272 (12.5)	20.586 (13.8)	23.696 (6.8)	9.7
$\ddot{u}_y$ (m/s^2)	Uncontrolled	6.1905	12.902	17.914	22.987	-
	40 LVDs	5.0244 (18.8)	8.5096 (34.0)	15.042 (16.0)	19.180 (16.6)	21.4
	40 NLVDs	5.4429 (12.0)	10.453 (19.0)	16.531 (7.7)	21.626 (5.9)	11.2
	20 LVDs	5.5026 (11.1)	10.020(22.3)	16.267 (9.2)	20.929 (9.0)	12.9
	20 NLVDs	5.4735 (11.6)	10.508 (18.6)	16.591 (7.4)	21.658 (5.8)	10.8
$\ddot{u}_\theta$ (rad/s^2)	Uncontrolled	0.0853	0.3126	0.2649	0.2429	-
	40 LVDs	0.0689 (19.2)	0.2036 (34.9)	0.2122 (19.9)	0.2069 (14.8)	22.2
	40 NLVDs	0.0756 (11.3)	0.2613 (16.4)	0.2367 (10.7)	0.2278 (6.2)	11.2
	20 LVDs	0.0755 (11.4)	0.2471 (21.0)	0.2342 (11.6)	0.2232 (8.1)	13.0
	20 NLVDs	0.0762 (10.6)	0.2626 (16.0)	0.2372 (10.5)	0.2283 (6.0)	10.8

(# The number written in the parenthesis represents the percentage reduction concerning uncontrolled response)

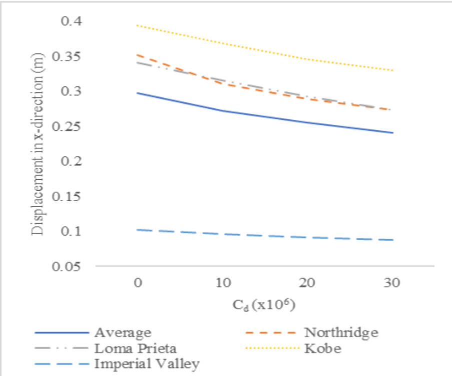

Fig. 7(a)

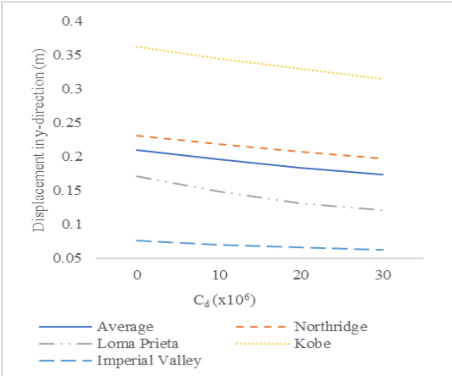

Fig. 7(b)

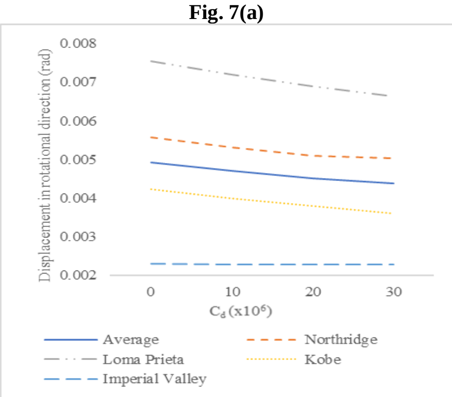

Fig. 7(c)

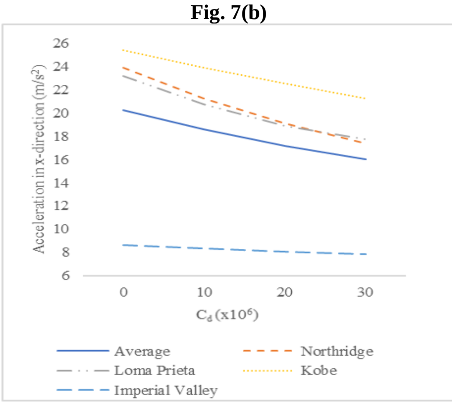

Fig. 7(d)

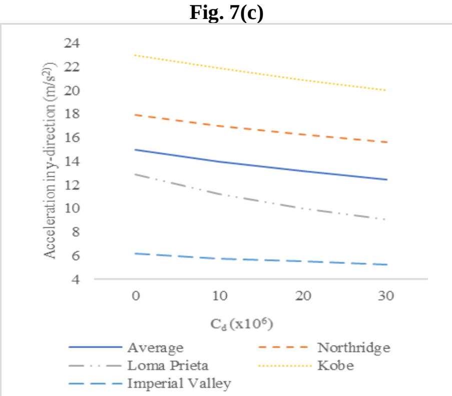

Fig. 7(e)

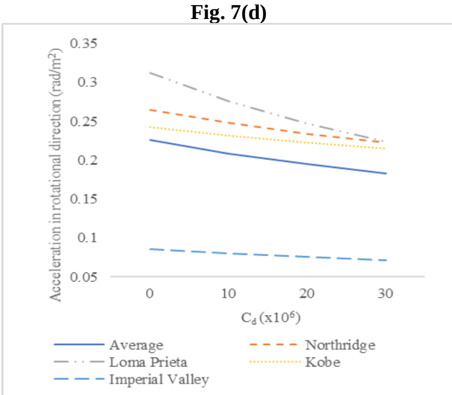

Fig. 7(f)

Fig. 7 Effect of C_d on response parameters for 20 LVDs

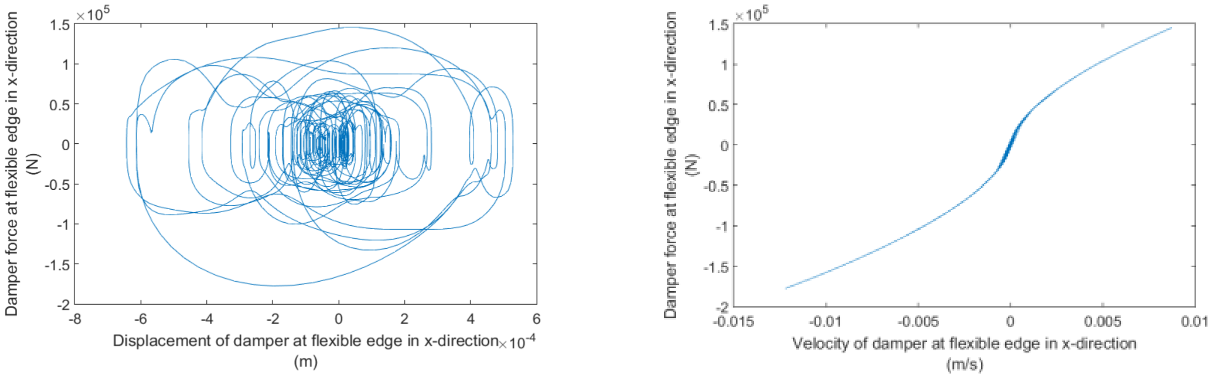

Fig. 8(a) Hysteresis loops for NLVDs located at the flexible edge at the top storey, having $C_d = 25 \times 10^5$ N-sec/m and $\alpha = 0.6$

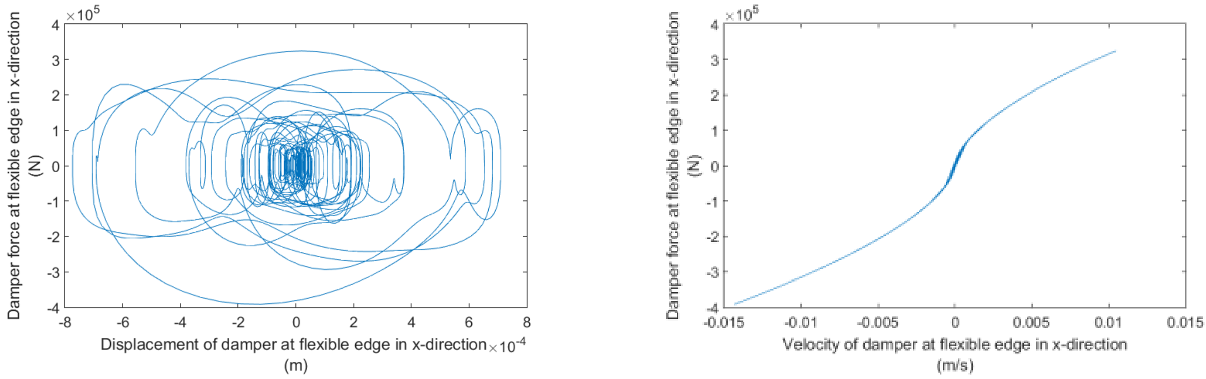

Fig. 8(b) Hysteresis loops for NLVDs located at the flexible edge at the top storey, having $C_d = 50 \times 10^5$ N-sec/m and $\alpha = 0.6$

Fig. 8 Hysteresis loops for Nonlinear Viscous Damper force-displacement and force-velocity for damper located at the flexible edge under Loma Prieta, 1989 earthquake. (a) Building configuration installed with 40 dampers (b) Building configuration installed with 20 dampers

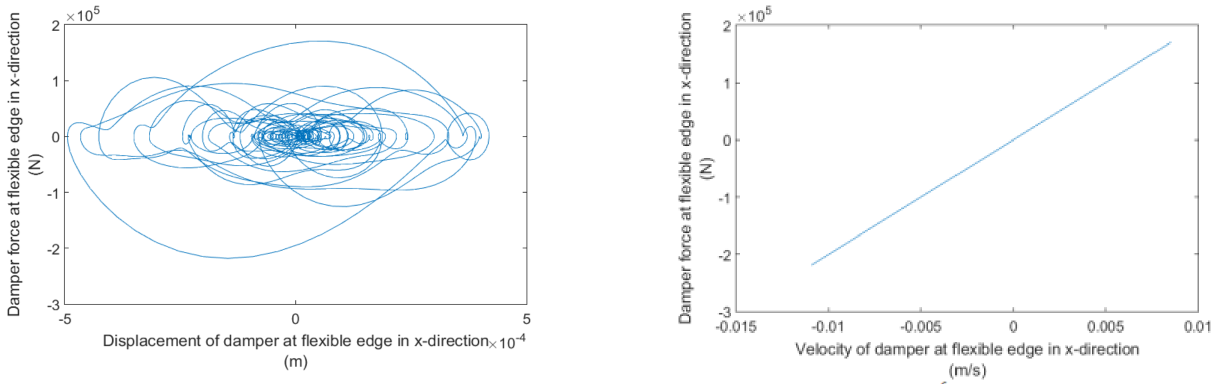

Fig. 9(a) Hysteresis loops for LVDs located at the flexible edge at the top storey, having $C_d = 20 \times 10^6$ N-sec/m and $\alpha = 1$

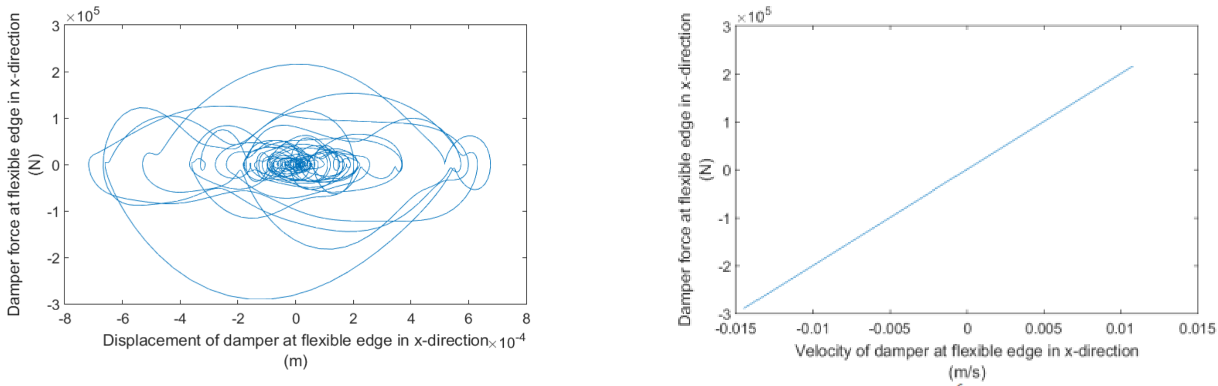

Fig. 9(b) Hysteresis loops for LVDs located at the flexible edge at the top storey, having $C_d = 20 \times 10^6$ N-sec/m and $\alpha = 1$

Fig. 9 Hysteresis loops for Linear Viscous Damper force-displacement and force-velocity for damper located at the flexible edge under Loma Prieta, 1989 earthquake. (a) Building configuration installed with 40 dampers (b) Building configuration installed with 20 dampers

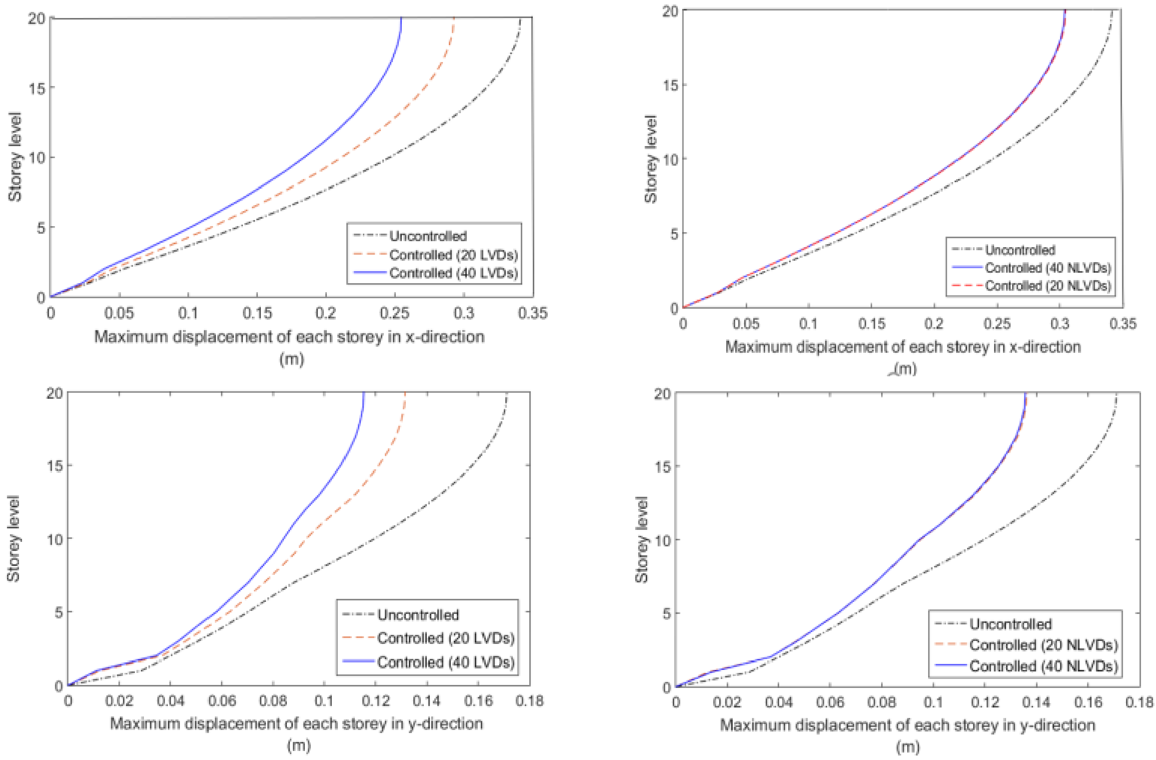

Fig. 10 Peak value of lateral displacement response of the structure in its uncontrolled and controlled state in x-direction and y-direction, under the Loma Prieta, 1989 earthquake

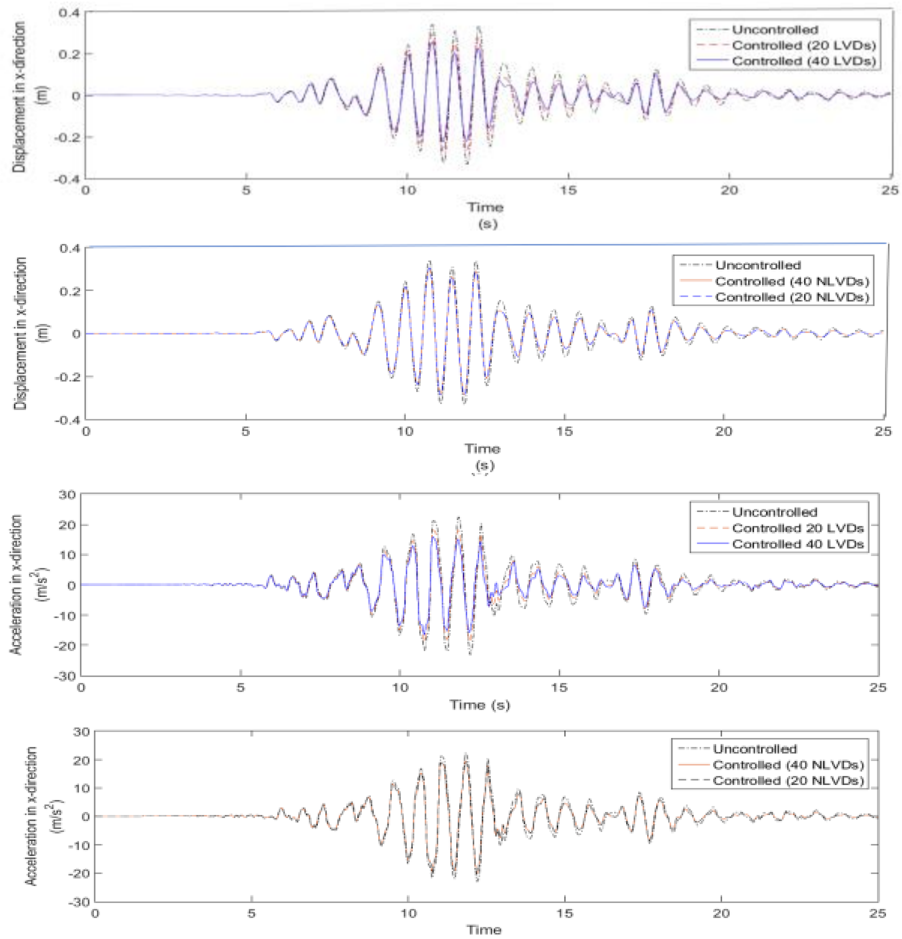

Fig. 11 Time history for comparison of controlled and uncontrolled displacement and acceleration response under Loma Prieta, 1989 earthquake

Table III represents values of various response parameters such as lateral displacement in the x-direction (u_x), lateral displacement in the y-direction (u_y), rotational direction (u_θ), lateral acceleration in the x-direction $(\ddot{u}_x)$, lateral acceleration in the y-direction $(\ddot{u}_y)$, rotational direction $(\ddot{u}_\theta)$. It is observed from Table III that, there is a significant difference in the reduction of response quantities for 40 LVDs and 20 LVDs, whereas the reduction is almost same for 40 NLVDs and 20 NLVDs. Further, it is noticed that less percentage reduction occurs in rotational displacement while installing both the types of viscous dampers into the building.

Fig. 10 shows the peak value of lateral displacements of the structure in its uncontrolled condition as well as when installed with LVDs, NLVDs under Loma Prieta, 1989 earthquake. As discussed earlier, significant change is seen while changing the number of dampers in the case of LVDs. Whereas in the case of NLVDs, almost similar behaviour is seen for both the configurations.

Fig. 11 shows the time history for uncontrolled and controlled displacement as well as acceleration response at 20th storey, using LVDs and NLVDs under Loma Prieta, 1989 earthquake. These time histories are plotted for LVDs and NLVDs, using the corresponding optimum parameters derived earlier. Further, similar trends are observed for the system under different earthquakes. Fig. 11 also shows the effectiveness of 40 and 20 LVDs as well as NLVDs in controlling displacement and acceleration responses.

VI. CONCLUSIONS

The seismic response of linearly elastic, 20 storied, two-way asymmetric building with non-linear viscous dampers and linear viscous dampers under bi-directional earthquake excitations is investigated. The responses are assessed with parametric variations to study the effectiveness of NLVDs and LVDs for the considered building. Two parameters are considered for NLVDs in the numerical study. Namely, the coefficient of damper (C_d) and exponent of velocity (α) and LVDs only coefficient of damper (C_d) is considered. From the present numerical study, the following conclusions can be made,

1. Generally, while studying the viscous dampers coefficient of the damper is kept the same for both NLVD as well as LVD. In the present study, a separate parametric study is carried out to obtain optimum parameters for NLVD and LVD. LVDs prove to be more effective as compared to NLVDs, based on suitable optimisation of damper parameters.
2. It is further observed that there is a significant difference in a reduction for various response quantities for 40 LVDs and 20 LVDs, whereas the reduction is almost same for 40 NLVDs and 20 NLVDs. Hence optimisation in the number of dampers can be achieved based on requirements for buildings.
3. The effectiveness of dampers depends on the dynamic properties of the building as well as on earthquake characteristics also.
4. Viscous dampers are found to be quite effective in reducing lateral-torsional displacement and acceleration responses.

REFERENCES

[1] IS 1893-Part 1, Indian Standard Criteria for Earthquake Resistant Design of Structures. 6.1. Bureau of Indian Standards, (2016).

[2] A. Bahnasy and O. Lavan, Linear or non-linear fluid viscous dampers? a seismic point of view., Bridging Your Passion with Your Profession - Proceedings of the 2013 Structures Congress, (2013) 2253-2264,

[3] M. Banazadeh, A. Ghanbari and R. Ghanbari, Seismic performance assessment of steel moment-resisting frames equipped with linear and non-linear fluid viscous dampers with the same damping ratio. Journal of Constructional Steel Research, 136(2017) 215–228.

[4] A. K. Chopra, Dynamics of Structures, Ed. 3rd. Pearson Publication, (1995).

[5] R. K. Goel, Effects of supplemental viscous damping on seismic response of asymmetric-plan systems. Earthquake Engineering and Structural Dynamics, 27(2)(1998) 25-141.

[6] R. K. Goel, Seismic response of linear and non-linear asymmetric systems with non-linear fluid viscous dampers. Earthquake Engineering and Structural Dynamics, 34(7) (2005) 825-846.

[7] G. C. Hart and K. Wong, Structural Dynamics for Structural Engineers, John Wiley and Sons, Inc., New York, 1999

[8] IS 16700, Criteria for Structural Safety of Tall Concrete Buildings, (2017).

[9] J. L. Lin and K. C. Tsai, Seismic analysis of two-way asymmetric building systems under bi-directional seismic ground motions. Earthquake Engineering and Structural Dynamics, 37(2008) 305-328,

[10] W. H. Lin and A. K. Chopra, Asymmetric one-storey elastic systems with non-linear viscous and viscoelastic dampers: simplified analysis and supplemental damping system design. Earthquake Engineering and Structural Dynamics, 32(4)(2003) 576-596.

[11] W. H. Lin and A. K. Chopra, Earthquake response of elastic SDF systems with non-linear fluid viscous dampers.Earthquake Engineering and Structural Dynamics, 31(9)(2002) 1623-1642.

[12] L. Y. Lu, Predictive control of seismic structures with semi-active friction dampers., Earthquake Engineering and Structural Dynamics, 33(5)(2004) 647-668

[13] M. Martinez-Rodrigo and M. L. Romero, An optimum retrofit strategy for moment resisting frames with non-linear viscous dampers for seismic applications., Engineering Structures 25(7) (2003) 913-925.

[14] N. S. Mehta and S. V. Mevada Seismic response of two-way asymmetric building installed with the hybrid arrangement of dampers under bi-directional excitations., International Journal of Structural Engineering, 8(3) 249-271.

[15] S. V. Mevada and R. S. Jangid, Seismic response of asymmetric systems with linear and non-linear viscous dampers., International Journal of Advanced Structural Engineering, 4(5)(2012) 1-20.

[16] Narayan B. Makwana, Snehal V. Mevada, Vishal B. Patel, Vibration Control of Asymmetric Building Subjected to Harmonic Excitation, SSRG International Journal of Civil Engineering 4(5) (2019) 75-78.

[17] T. T. Soong, and G. F. Dargush, Passive Energy Dissipation Systems in Structural Engineering., John Willey and Sons, Inc., Newyork, (1997).